



Exchange of sea ice between the Arctic Ocean and the Canadian Arctic Archipelago

Ron Kwok¹

Received 5 June 2006; revised 7 July 2006; accepted 12 July 2006; published 18 August 2006.

[1] First estimates of sea ice exchange between the Arctic Ocean and the Canadian Arctic Archipelago (CAA) are obtained using six years (1997–2002) of RADARSAT ice motion. Over the period, the mean annual flux of sea ice area from the Amundsen Gulf (AG), M'Clure Strait (MS), and Queen Elizabeth Islands (QEI) are $-85 \pm 26 \times 10^3$, $-20 \pm 24 \times 10^3$, and $8 \pm 6 \times 10^3$ km². Positive/negative sign indicates Arctic outflow/inflow. Overall, net sea ice area is exported from the CAA; rough estimates suggest a mean annual volume flux of $\sim 10^2$ km³ into the Canada Basin. Ice types are largely seasonal near the AG flux gate, mixed seasonal and multiyear at the MS gate, and primarily multiyear at the QEI gates. Sea ice at the QEI flux gates remains land fast for most of the year. Cross-strait gradient in sea level pressure explains more than 50% of the variance in the area flux at these passages. The role of ice exchange during the anomalous decrease in multiyear ice coverage in the Sverdrup Basin during September 1998 is examined.

Citation: Kwok, R. (2006), Exchange of sea ice between the Arctic Ocean and the Canadian Arctic Archipelago, *Geophys. Res. Lett.*, 33, L16501, doi:10.1029/2006GL027094.

1. Introduction

[2] Excluding Nares Strait, the passages between the Canadian Arctic Archipelago (CAA) and the Arctic Ocean span a latitude range of 12° from 70°N and thus a range of ice and climate conditions. Existing information concerning the sea ice and climate conditions of the Sverdrup Basin (the marine area of the CAA north of Parry Channel) is well summarized by *Melling* [2002]. The sea ice cover within this basin is primarily multiyear or second year, with an average thickness of in the late winter of 3.4 m, and is land fast for more than half the year. The navigability of the Northwest Passage - a potential deepwater shortcut for shipping between the Atlantic and the Pacific - is thought to be affected by heavy multiyear ice formed here as well as the Arctic Ocean to the west. To the south, the sea ice conditions/climatology of the Amundsen Gulf (AG) and M'Clure Strait (MS) seem to have received less attention: little focused work is available in the published literature except for the two submarine surveys of the M'Clure Strait ice cover in the 1960s [*McLaren et al.*, 1984]. Broadly, the MS ice cover contains a mix of first-year and multiyear ice while the AG ice cover is generally first-year and produced locally. From time to time there are incursions of old ice, potentially from the Sverdrup Basin/Arctic Ocean, into

these areas in mid to late summer. A recent large-scale study of the southern Beaufort [*Barber and Hanesiak*, 2004] reports significant negative trends in ice concentration anomalies in both the AG and MS between 1979 and 2000.

[3] While it is generally accepted that there are modest exchanges of sea ice between the Canadian Arctic Archipelago (CAA) and the Arctic Ocean, they have never been quantified. Changes in Arctic climate may influence the ice conditions and exchange rates that could have unforeseen consequences. The present note seeks to establish a first baseline estimate of the ice area exchanges between the CAA and Arctic Ocean using a 6-year record (1997–2002) of RADARSAT ice motion. The connection of these exchanges to atmospheric forcing is explored. Based on available ice thickness estimates, rough volume exchanges are estimated.

2. Data Description

[4] The primary data sets include: 1) ice motion from RADARSAT; 2) ice concentration estimates from satellite passive microwave data; and, 3) daily sea level pressure fields from the NCEP-NCAR products [*Kalnay et al.*, 1996].

[5] Ice exchanges between the Arctic Ocean and Canadian Archipelago are estimated at seven flux gates placed near the openings into the: (a) Amundsen Gulf; (b) M'Clure Strait; (c) Ballantyne and Wilkins Straits, and Prince Gustaf Adolf Sea; (d) Peary and Sverdrup Straits. Their locations and widths are shown in Figure 1. Henceforth, the gates that connect the western Arctic Ocean and the Sverdrup Basin (SB), i.e., (c) and (d), will be referred to collectively as QEI-South and QEI-North.

[6] Ice motion is derived from RADARSAT SAR imagery (spatial resolution: ~ 150 m) by computing the displacement of common ice features in time-separated images using an image matching procedure described by *Kwok et al.* [1990]. Between 1997 and 2002, the available repeat coverage of the CAA passages is nominally 3 days although a small fraction of motion estimates are over a longer period. The 3-day ice motion is sampled on a 5-km grid that covers a region of ~ 30 km on each side the gate. All motion vectors are visually inspected for quality and corrected or replaced where needed.

[7] Area flux is computed by first interpolating the gridded ice motion to the gate and then integrating the gate-perpendicular component of the motion profile using the trapezoidal rule. The motion profile is constrained to go to zero at the coastal endpoints. The area flux is weighted by satellite ice concentration. The expected uncertainty in the displacement estimates is ~ 300 m. If we assume that the errors of the motion samples are additive, unbiased, uncorrelated and normally distributed, the uncertainties in the area flux over any given time interval, σ_F , can be computed

¹Jet Propulsion Laboratory, California Institute of Technology, Pasadena, California, USA.

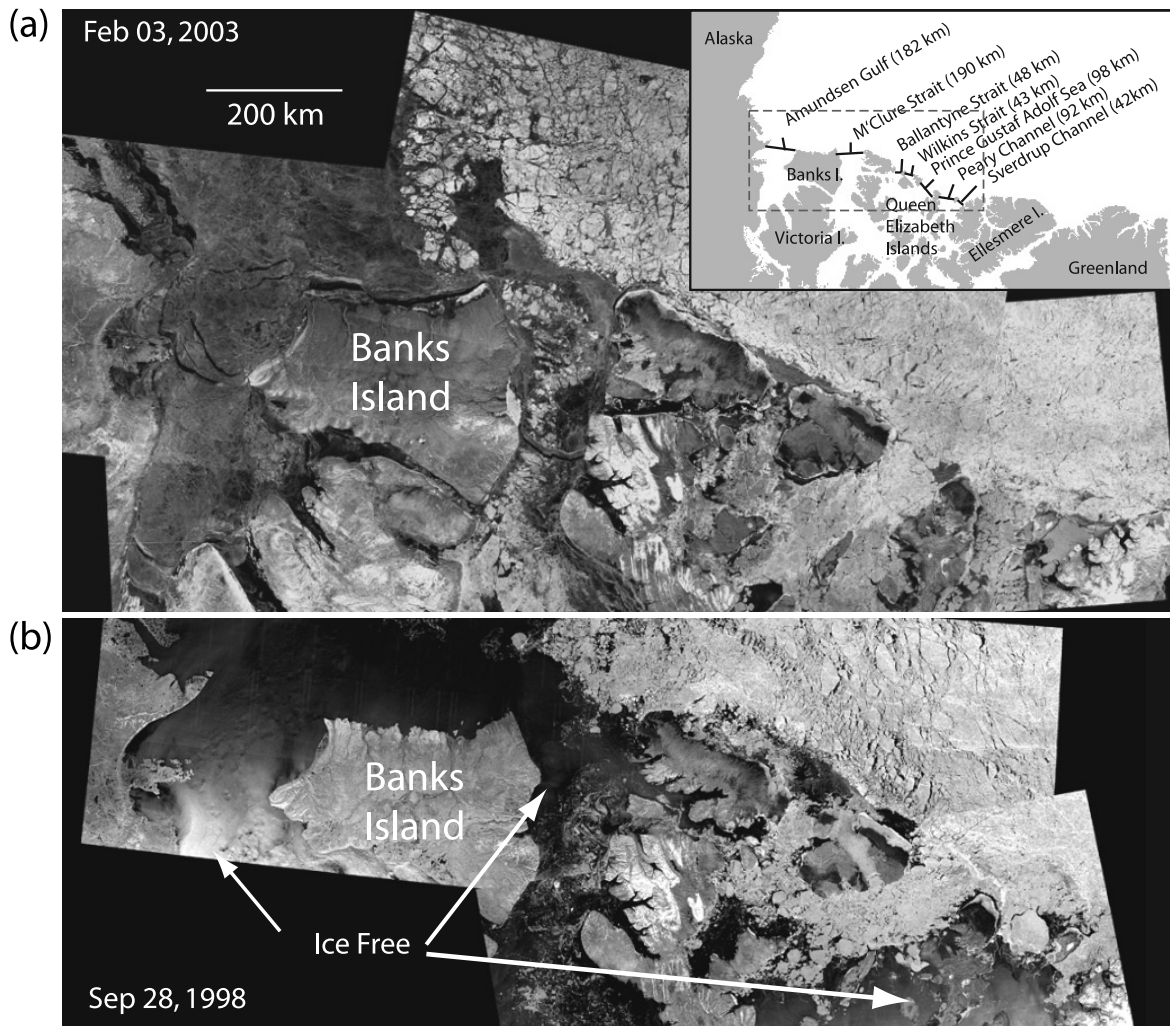


Figure 1. RADARSAT imagery shows the ice conditions adjacent to the flux gates during (a) the winter of 2003 (February 3) and (b) summer of 1998 (September 28). Inset shows width and location of the flux gates. Dashed rectangle shows the coverage of the first image. Arrows point to ice free areas (RADARSAT imagery ©CSA 2004).

viz. [Kwok and Rothrock, 1999]: $\sigma_F = \sigma_u L / \sqrt{N_s}$, where L is the width of the flux gate, σ_u is the standard error in the displacement estimates and N_s is the number of independent samples. For a 100 km gate, say $N_s = 20$ (number of 5 km samples along the gate) and $\sigma_u = 300$ m, the uncertainty in area flux is only ~ 7 km² over the sampling interval.

[8] Winter ice conditions (November through April) at the passages are characterized by the coverage of first-year (FY) and multiyear (MY) ice 50 km on the archipelago side of the flux gates; this provides a better sampling of the ice conditions in the CAA. Ice types are from a backscatter-based procedure [Kwok et al., 1992] that classifies each RADARSAT SAR image pixel as a member of one of these two types. Broad assessments of the quality of these estimates [Kwok and Cunningham, 2002] have shown this approach to be relatively robust during the winter.

3. Results and Discussion

3.1. Area and Volume Flux

[9] Figure 2 shows the time series of monthly area exchange and multiyear ice fraction at the Amundsen Gulf,

M'Clure Strait, QEI-South and QEI-North flux gates. The annual area flux through these gates is shown in Figure 3. Positive/negative sign indicates Arctic outflow/inflow.

3.1.1. Amundsen Gulf (AG)

[10] The 182 km flux gate at the AG is located between the mainland and southwestern tip of Banks Island. The ice cover across this southern most gate is almost entirely seasonal (Figure 2a) and suggests that most of the ice is either exported or breaks up and melts through the spring and summer. In fact, five of the six years shown here saw at least one month of ice-free conditions during the summer (Figure 2a). At the flux gate, more than five months of the spring and summer (June through October) are ice-free in 1998. Open water coverage can be clearly seen in the end-of-September RADARSAT image (Figure 1b). The average annual ice area flux is -85×10^3 km² and ranges from -113×10^3 km² in 1998 to -44×10^3 km² in 2000. Ice flux is predominantly into the Beaufort Sea and largely during the fall and winter (Figures 2a and 2e). Much of the ice production in the fall and winter can be attributed to the activity of the Cape Bathurst Polynya. Unlike the flux gates discussed below, we are not aware of any published

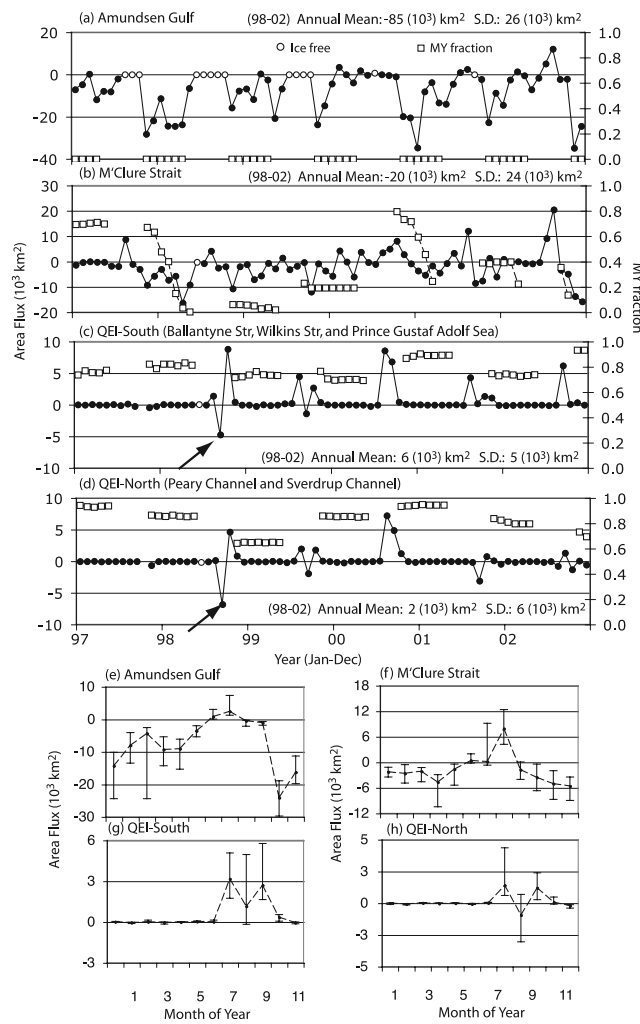


Figure 2. Time series of monthly (1997–2002) ice area flux (solid circles) and multiyear ice fraction (squares) estimates. (a) Amundsen Gulf. (b) M’Clure Strait. (c) Ballantyne Strait, Wilkins Strait, and passage into Prince Gustaf Adolf Sea. (d) Peary and Sverdrup Channels. (e–h) Monthly variability over the period. Open circles indicate months that are ice-free. Note the data gap in Oct 1997. Positive/negative sign indicates Arctic outflow/inflow. Arrows point to the extremes in September of 1998.

estimates of ice thickness at the AG. Assuming a mean seasonal ice thickness of ~1–1.5 m, we estimate a mean annual ice export into the Arctic of ~85–130 km³.

3.1.2. M’Clure Strait (MS)

[11] This strait connects the Beaufort Sea in the west with Viscount Melville Sound in the east. This ~190 km opening into the Arctic Ocean is bounded by Prince Patrick Island to the north and Banks Island to the south. At the gate, the ice type coverage is largely FY but MY ice is also found through most of the year (Figure 2b). The mix of ice types is more variable in some years compared to others. In summer, the only year where ice-free conditions persisted for at least a month is 1998. The annual mean ice flux of $-20 \times 10^3 \text{ km}^2$ ranges from $-55 \times 10^3 \text{ km}^2$ in 1998 to $15 \times 10^3 \text{ km}^2$ in 2000. In the mean, sea ice is exported into the Arctic Ocean; 2000 is the only year when there is net sea

ice import from the Arctic Ocean. McLaren *et al.* [1984] report a mean draft of 4–5 m of mainly first year ice within M’Clure Strait; this is from an under-ice profiling sonar operated during two submarine surveys in February and August of 1960. Contemporary ice thickness estimates are not available. Taking the sea ice to be 4 m thick, the annual mean ice volume export into the Arctic Ocean would be 80 km³. The uncertainty in this estimate is high: we suspect that this may not be representative of current ice thickness in the Strait considering the observed thinning in Arctic sea ice during the past 40 years [Rothrock *et al.*, 1999]. We speculate that half of that volume seems more reasonable but would indicate significantly thinning here.

3.1.3. QEI-South

[12] This includes the flux gates into the Ballantyne and Wilkins Straits, and Prince Gustaf Adolf Sea. The adjacent ice cover is primarily made up of old ice (~80% MY ice coverage). Over the five years (98–02), the annual mean ice area flux of $6 \pm 5 \times 10^3 \text{ km}^2$ through these three gates, with a net width of 189 km, is relatively small. This is only a fraction of the area exchange at the AG and MS. Thick multiyear ice is imported from the Arctic Ocean through mainly the passage into the Prince Gustaf Adolf Sea. The sea ice in the QEI remains land fast for most of the year (from December through June – see Figures 2c and 2g). Using drill hole measurements from the 1970s, Melling [2002] reports a mean ice thickness of ~3.4 m in the northern CAA or Sverdrup Basin. Again, these are not contemporary ice thickness estimates. But, taking this to be the mean thickness we estimate the mean ice volume flux from the Arctic Ocean into the QEI-South gates to be ~20 km³.

3.1.4. QEI-North

[13] This includes exchanges at the two flux gates (134 km wide) into the Peary Channel in the south and Sverdrup Channel in the northern QE Islands. The ice cover is primarily of old ice. The ice flux is smallest compared to the above gates and has a net annual mean of $2 \pm 6 \times 10^3 \text{ km}^2$. Thick multiyear ice is imported from the Arctic Ocean with higher ice flux at the wider Peary Channel.

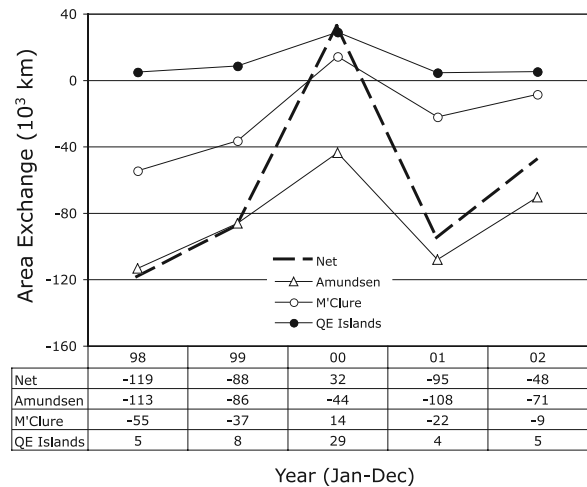


Figure 3. Annual ice area flux (1998–2002) at the Amundsen, M’Clure, and Queen Elizabeth Islands flux gates. 1997 is not included because of the data gap in Oct 1997. Positive/negative sign indicates Arctic outflow/inflow.

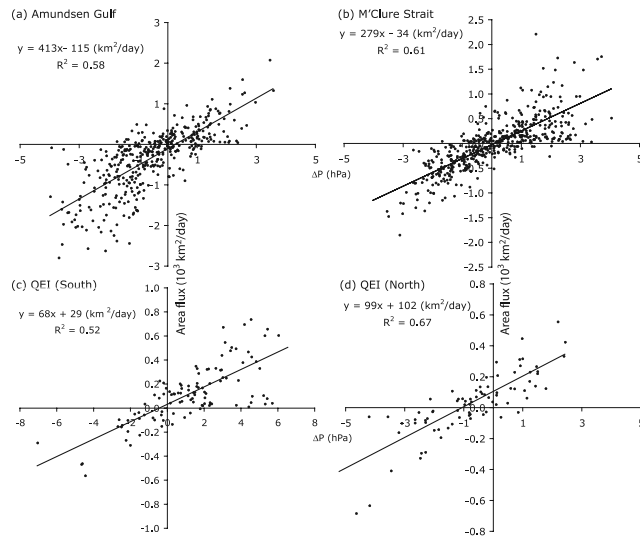


Figure 4. Scatterplot of daily ice flux and cross-gate pressure gradient (ΔP). (a) Amundsen Gulf. (b) M'Clure Strait. (c) QEI-South. (d) QEI-North. Periods when the ice is land fast (i.e., no motion) are excluded by removing estimates that are $<100 \text{ km}^2/\text{day}$.

Using the same 3.4 m as the mean ice thickness, we find the mean ice flux of $\sim 7 \text{ km}^3$ from the Arctic Ocean into the northern Sverdrup Basin to be quite small. The inflow of Arctic sea ice into the QE Islands supports the argument [Melling, 2002] that the thick modes he observed in the thickness histograms in the Sverdrup Basin originates from the zone of heavy ridging along the periphery of the Beaufort gyre. The thick modes appear chiefly in the northern parts of Prince Gustaf Adolf Sea, MacLean Strait and Danish Strait. These channels provide the least obstructed routes for the southward drift of ice from the Arctic coast.

3.1.5. Net Area and Volume Flux

[14] Over the 6-year period, Figure 3 shows that the CAA contributes net sea ice area to the Arctic Ocean, primarily through Amundsen Gulf and M'Clure Strait. The net inflow of Arctic sea ice area into the QE Islands is quite small (mean $<10 \times 10^3 \text{ km}^2$) compared to the marine area of the QE Islands (Sverdrup Basin) of $\sim 243 \times 10^3 \text{ km}^2$. Perhaps of more interest is the net annual flux of sea ice volume. Our mean annual estimates are: -85 to -130 km^3 (AG), -80 km^3 (MS), $+27 \text{ km}^3$ (QEI-North and South). Volume flux at the AG and MS are significantly higher than at the QEI gates. Even though the uncertainties in these estimates are high due to lack of contemporaneous ice thickness measurements, it seems clear from their relative magnitudes that the ice produced in the CAA, albeit small, adds $\sim 10^2 \text{ km}^3$ to the ice volume of the Arctic Ocean.

3.2. Area Flux and Cross-Gate Gradient in Sea Level Pressure

[15] Since ice motion is largely wind-driven and is nearly parallel to isobars of sea level pressure (SLP), we examine the response of sea ice area flux to cross-gate pressure gradients (ΔP) at the CAA gates. We define this gradient to be the difference in SLP between the two terminals of a flux gate. The gradient is computed such that positive/negative

values correspond to Arctic outflows/inflows. Results of the regression between the two variables are shown in Figure 4. Periods when the ice is land fast (i.e., no motion) are excluded by removing estimates that are $<100 \text{ km}^2/\text{day}$. For the four gates examined here, ΔP explains between 52% and 67% of the variances in ice area exchanges between the Arctic Ocean and the CAA. When the ice is not land fast, the linear equations (Figure 4) are reasonable predictors of ice flux. Differences in the magnitude of the regression slopes provide an indication of the local sea ice interactions and regional ice thickness. For example, even though the widths of the AG and MS flux gates are similar, the larger regression slope at the AG can be attributed mainly to the thinner ice cover in the AG with near free-drift conditions in late spring and early fall. The regression slopes at the QEI-North and QEI-South gates are more than 3–5 times smaller than the southern gates, and that is likely related to the thicker and more compact Arctic Ocean and QEI ice cover in the vicinity of these gates. Though there is a preferred direction of annual net flow at each gate, it can be seen that there is frequent area exchanges (inflow/outflow) by the distribution of points in first and third quadrants of the scatterplot.

3.3. Anomalies in 1998

[16] Jeffers *et al.* [2001] and Agnew *et al.* [2001] document an unusual breakup of the old multiyear fast-ice plug in Sverdrup Channel during the summer of 1998. In particular, Jeffers *et al.* [2001] argue that the widespread loss of multiyear ice in 1998 can be attributed in part to air temperature that was 2.5°C warmer than normal that summer. Here, we examine the role of ice exchange between the Arctic Ocean and Sverdrup Basin during this time. The ice conditions at the end of September 1998 can be seen in the RADARSAT SAR image (Figure 1b): the Peary and Sverdrup Channels, north of Ellef Ringnes Island are largely ice free; the Arctic ice cover just west of these channels, however, remains fairly compact. In response to a September SLP field with a high centered over Greenland, the direction of ice movement is toward the Arctic Ocean. In fact, the month of September saw the largest export of sea ice ($10 \times 10^3 \text{ km}^2$) from the Sverdrup Basin (SB) into the Arctic Ocean over the 6-year period. This extreme in ice export explains about one-third of the observed ice-free area of $>30 \times 10^3 \text{ km}^2$ [Melling, 2002] during that time. In addition to ice melt, consideration should also be given to ice export through the channels/straits to the south of SB but this is not within the scope of the present examination. It is also interesting to note that there is an influx of Arctic sea ice of $\sim 14 \times 10^3 \text{ km}^2$ the following October. Even with this replenishment of old ice in the SB, the following winter saw a significant decrease in MY coverage (Figure 2d) at the Peary and Sverdrup Channel, only returning to its previous levels in the next winter.

4. Conclusions

[17] The present note examines a 6-year record of sea ice area exchange between the Arctic Ocean and CAA from high resolution RADARSAT ice motion. Routine high-resolution SAR coverage provides the capability to monitor the ice drift accurately in the narrow channels of the

Canadian Arctic Archipelago. Over the period, the mean annual flux of sea ice area from the AG, MS and QEI are $-85 \pm 26 \times 10^3$, $-20 \pm 24 \times 10^3$, and $+8 \pm 6 \times 10^3$ km². This establishes a baseline for future comparisons. Overall, there is net outflow of sea ice area from the CAA. Our rough estimates suggest an annual mean volume export of $\sim 10^2$ km³ of sea ice to the Arctic Ocean. This can be compared to the mean annual ice volume flux of ~ 130 km³ at Nares Strait [Kwok, 2005] and at Fram Strait of ~ 2000 km³ [Kwok *et al.*, 2004a]. Most of this volume is exported to the Canada Basin during the winter and spring; the impact of this volume flux on Arctic Ocean circulation and hydrography remains to be explored.

[18] From the perspective of Arctic sea ice export into Baffin Bay, the negligible inflow of Arctic sea ice at the CAA gates considered here suggests that the sea ice exported into Baffin Bay, except for the contribution from Nares Strait, is produced almost entirely within the CAA with minor contributions from the Arctic. It is also important to recognize that this relatively short 6-year sampling may not be adequate to sample intermittent events of Arctic ice influx that may occur at longer timescales.

[19] In the past, it has been suggested that the Northwest Passage is minimally used because of the inflow of heavy multiyear ice from the Arctic Ocean in the west and the Sverdrup Basin in the north. We show, during the 6-year period examined here, the inflow of Arctic Ocean sea ice does not seem to be a factor. But, this could be associated with changes in the climate of the Arctic during the past decade.

[20] Certainly, with the continuation of the RADARSAT program, we are now in a position to monitor these exchanges on a routine basis. The availability of ICESat [Kwok *et al.*, 2004b] and other radar altimeters [Laxon *et al.*, 2003] would allow us to better estimate the thickness distribution and assess the sea ice changes in straits and passages of the Canadian Arctic Archipelago.

[21] **Acknowledgments.** I wish to thank S. S. Pang for her assistance during the preparation of this manuscript. RADARSAT images are provided by the Alaska Satellite Facility, Fairbanks, Alaska. This work was

performed at the Jet Propulsion Laboratory, California Institute of Technology, and is sponsored by the National Science Foundation and the National Aeronautics and Space Administration.

References

- Agnew, T., B. Alt, R. De Abreu, and S. Jeffers (2001), The loss of decades old sea ice plugs in the Canadian Arctic Islands, paper presented at 6th Conference on Polar Meteorology and Oceanography, Am. Meteorol. Soc., San Diego, Calif.
- Barber, D. G., and J. M. Hanesiak (2004), Meteorological forcing of sea ice concentrations in the southern Beaufort Sea over the period 1979 to 2000, *J. Geophys. Res.*, *109*, C06014, doi:10.1029/2003JC002027.
- Jeffers, S., T. Agnew, B. Alt, R. De Abreu, and S. McCourt (2001), Investigating the anomalous sea ice conditions in the Canadian High Arctic (Queen Elizabeth Islands) during the summer of 1998, *Ann. Glaciol.*, *33*, 507–612.
- Kalnay, E., et al. (1996), The NCEP/NCAR 40-year reanalysis project, *Bull. Am. Meteorol. Soc.*, *77*, 437–471.
- Kwok, R. (2005), Variability of Nares Strait ice flux, *Geophys. Res. Lett.*, *32*, L24502, doi:10.1029/2005GL024768.
- Kwok, R., and G. F. Cunningham (2002), Seasonal ice area and volume production of the Arctic Ocean: November 1996 through April 1997, *J. Geophys. Res.*, *107*(C10), 8038, doi:10.1029/2000JC000469.
- Kwok, R., and D. A. Rothrock (1999), Variability of Fram Strait flux and North Atlantic Oscillation, *J. Geophys. Res.*, *104*(C3), 5177–5189.
- Kwok, R., J. C. Curlander, R. McConnell, and S. Pang (1990), An ice motion tracking system at the Alaska SAR Facility, *IEEE J. Oceanic Eng.*, *15*(1), 44–54.
- Kwok, R., E. Rignot, B. Holt, and R. G. Onstott (1992), Identification of sea ice type in spaceborne SAR data, *J. Geophys. Res.*, *97*(C2), 2391–2402.
- Kwok, R., G. F. Cunningham, and S. S. Pang (2004a), Fram Strait sea ice outflow, *J. Geophys. Res.*, *109*, C01009, doi:10.1029/2003JC001785.
- Kwok, R., H. J. Zwally, and D. Yi (2004b), ICESat observations of Arctic sea ice: A first look, *Geophys. Res. Lett.*, *31*, L16401, doi:10.1029/2004GL020309.
- Laxon, S., N. Peacock, and D. Smith (2003), High interannual variability of sea ice in the Arctic region, *Nature*, *425*, 947–950.
- McLaren, A. S., P. Wadhams, and R. Weintraub (1984), The sea ice topography of M'Clure Strait in winter and summer of 1960 from submarine profiles, *Arctic*, *37*(2), 110–120.
- Melling, H. (2002), Sea ice of the northern Canadian Arctic Archipelago, *J. Geophys. Res.*, *107*(C11), 3181, doi:10.1029/2001JC001102.
- Rothrock, D. A., Y. Yu, and G. A. Maykut (1999), Thinning of the Arctic sea-ice cover, *Geophys. Res. Lett.*, *26*(23), 3469–3472.

R. Kwok, Jet Propulsion Laboratory, California Institute of Technology, 4800 Oak Grove Drive, Pasadena, CA 91109, USA. (ron.kwok@jpl.nasa.gov)